

**Pentacyclic Triterpenoids from *Combretum platypetalum* subsp. *oatesii* (Rolfe) Exell (*Combretaceae*) Root Inhibit Sterol 14 α -Demethylase Target**Sampson D. Umoh^{1,2}, Gomotsang Bojase^{1*}, Ishmael B. Masesane¹, Runner T. Majinda¹, Daniel Loeto³, Taye B. Demissie¹¹Department of Chemistry, Faculty of Science, University of Botswana, Gaborone, Botswana²Department of Chemistry, College of Physical Sciences, Joseph Sarwuan Tarka University, Makurdi, formerly known as Federal University of Agriculture, Makurdi Nigeria³Department of Biological Sciences, Faculty of Science, University of Botswana, Gaborone, Botswana

ARTICLE INFO

ABSTRACT

Article history:

Received 10 August 2023

Revised 11 December 2023

Accepted 13 December 2023

Published online 01 January 2024

Copyright: © 2023 Umoh *et al.* This is an open-access article distributed under the terms of the [Creative Commons Attribution License](https://creativecommons.org/licenses/by/4.0/), which permits unrestricted use, distribution, and reproduction in any medium, provided the original author and source are credited.

The *Combretum* genus, with its few investigated members, has shown evidence-based justification for its extensive study in finding natural alternatives to various maladies. One of its species, *Combretum platypetalum*, has been traditionally used to treat diarrhea, pneumonia, dysmenorrhea, and infertility in women, with phytochemical investigations focusing on its leaves. The plant part(s) employed in the traditional practice are not explicitly mentioned in the literature, but several therapeutic properties have been confirmed. This study is a follow-up to previous metabolomic reports and a comprehensive biological investigation of the root extract, aimed at investigating the active compounds. The root was extracted by maceration, and compounds were isolated using various chromatographic techniques. Combrenorplatypta A, arjunolic acid, betulinic acid, and lupeol (2-4) were bioguidedly isolated from *C. platypetalum* root for the first time. The structures of the isolated compounds were established based on spectroscopic (1D NMR, 2D NMR, IR, UV, and ECD) and spectrometric (ESIMS) data as well as time-dependent density functional theory (TD-DFT) calculations. *In vitro* and computational antifungal activities of the compounds were investigated; after that, molecular docking analysis of structures (1-4) versus target (sterol 14 α - demethylase) binding affinity for druggability was established. The MICs of *in vitro* bio-investigated compounds ranged from 2.30 μ M to 15 μ M, while computational antifungal investigations showed MICs from 4 nM to 49.86 nM. The compounds produced over six times the activity of fluconazole, a first-line antifungal drug. This study has identified the active sites and possible mechanisms of action of molecules against fungal pathogens.

Keywords: Antifungal, Biological activity, *Combretum platypetalum*, Sterol 14 α -demethylase, Triterpenoids

Introduction

Mortality rates accrued from fungal infections have consistently increased,^{1,2} and resistance to synthetic azole antifungal agents is presently a cause for concern.³ The present investigation identified sterol 14 α - demethylase as the target site in the search for new antifungal agents from natural sources. The fungal cell wall is highly dependent on the biosynthesis of ergosterol,⁴ which gives it the required rigidity to protect the cell contents. On the other hand, ergosterol is synthesized from squalene.⁵ Squalene is converted to lanosterol through squalene epoxidase.⁶ With the help of the sterol 14 α - demethylase, a cytochrome P450 enzyme (CYP51), lanosterol is demethylated at carbon 14(α) via some intermediates to produce ergosterol.⁷ The inhibition of the sterol 14 α - demethylase leads to the accumulation of methylated sterol precursors⁴ and a deficiency of ergosterol, leading to the depletion of the fungal cell membrane and subsequent cell death.

*Corresponding author. E mail: bojaseg@ub.ac.bw
Tel: +267 74305431

Citation: Umoh SD, Bojase G, Masesane IB, Majinda RT, Loeto D, Demissie TB. Pentacyclic Triterpenoids from *Combretum platypetalum* subsp. *oatesii* (Rolfe) Exell (*Combretaceae*) Root Inhibit Sterol 14 α -Demethylase Target. Trop J Nat Prod Res. 2023; 7(12):5441-5447. <http://www.doi.org/10.26538/tjnpr/v7i12.12>

Official Journal of Natural Product Research Group, Faculty of Pharmacy, University of Benin, Benin City, Nigeria.

Azole antifungal agents are sterol 14 α -demethylase inhibitors.⁴ This guided our search for antifungal agents from *Combretum* species used over the years in the treatment of fungal-related infections by African traditional healers.

The bioguided isolation approach was used in the study of *Combretum platypetalum* subsp. *oatesii* (Rolfe) Exell (*Combretaceae*), overcoming the challenge of random isolation of inactive compounds, which has characterized most natural product drug discovery programs. The investigated species is a dwarf shrub peculiar to Western and Southern Africa. It is locally known as the red wing, which translates as *adaidad mba* in the Annang local dialect of Nigeria or *motserwe* in Setswana. In the African traditional medicine system, *C. platypetalum* is used in the treatment of several infectious and non-infectious diseases.⁸ However, the plant part used in the traditional treatment is not explicitly stated in the literature.⁸ The species' phytochemical investigation has identified three compounds from the leaves,^{9,10} but no compounds from its stem or root have been reported, except for the metabolomic identification of non-volatile bioactive constituents by Majinda and co-workers.⁸ The literature survey reveals a diverse range of extraction solvents and methods used in studying the genus.¹¹ This paper aims to identify potential antifungal lead compounds from *C. Platypetalum* and for the first time, we describe the bioguided isolation of compounds (1-4) from *Combretum platypetalum* root. The study reports on the *in vitro* and computational antifungal activities of the isolated compounds, and their molecular docking for druggability against the sterol 14 α - demethylase fungal target site and gives directions for future investigations.

Materials and Methods

General Experimental Procedures

A Rudolph Research Analytical Polarimeter (Rudolph Research Analytica Corporation, 354, Route 206, Flanders, NJ 07836 USA) was used to determine optical rotation. UV spectra were measured on a Thermo Scientific Evolution 201 UV-Visible Spectrophotometer. IR spectra were recorded using the PerkinElmer FT-IR spectrometer (PerkinElmer, Inc.). The ECD spectrum was acquired using the Jasco model J-180 spectropolarimeter (Jasco Corporation, 2967-5, Ishikawacho, Hachioji, Tokyo, Japan). NMR spectra were recorded using (a) Bruker Avance 400 and 101 MHz and (b) Bruker Ascend 500 and 126 MHz for proton and carbon, respectively (Bruker, Switzerland AG, Industriestrasse 26, CH-8117 Fallanden) using deuterated solvents for NMR analysis and TMS as references. ESIMS data was obtained using a low-resolution mass spectrometer. Column chromatography (CC) was carried out using silica gel 60 (0.040-0.063 mm), and preparative TLC was carried out using silica gel 60 HF₂₅₄₊₃₆₆ precoated on 20 cm × 20 cm glass plates with a thickness of 0.75 mm and Sephadex LH20. Sartorius analytical balance (BCE2241-1S), Germany, with an accuracy of 0.1mg, was used. The extraction of plant materials was performed using distilled general-purpose-grade solvents, while all other analytical work was conducted using analytical-grade solvents (with percentage purities ≥ 95%) from Sigma-Aldrich without further purification.

Collection and Authentication of Plant Material

Parts of *C. platyptalum* were collected during the rainy season (September 2013) at the Faculty of Science, University of Ibadan, Nigeria. The sample collection site is located 5 kilometers north of Ibadan, Nigeria, at latitude 7° 25' north, longitude 3° 54' east, and a mean altitude of 221 m above sea level. The annual rainfall is roughly 1220 mm (48"), raining between April and October. The Forestry Research Institute of Nigeria (FRIN) authenticated the species and deposited a herbarium sample (FHI Number 109750).

Extractions from *Combretum platyptalum*

The root of *C. platyptalum* was air-dried and pulverised with a Thomas Scientific Model 4 Willey mill (Swedesboro, NJ, USA), and 1.40 kg of pulverised plant material was obtained. Extraction was done by maceration with 100% *n*-hexane, dichloromethane: methanol (1:1), and 100% methanol, respectively, to afford 6 mL of oil from 100% *n*-hexane extraction, 25.4602 g of extract from DCM: MeOH, and 30.1098 g of extract from 100% MeOH extraction.

Isolation of Compounds from *Combretum platyptalum* Root

The methanol extract of the root (30.1098 g) was chromatographed over a silica gel column with *n*-hexane, ethyl acetate, and methanol at a 10% polarity increment of 250 mL each to produce 21 fractions. Based on TLC analysis, the fractions were pooled to make four sub-fractions (F₁ – F₄). The fractions were biologically investigated, and fractions F₂ (4.9104 g) and F₃ (20.6800 g) produced the highest antifungal activity. Further investigation of fractions F₁ (750 mg) and F₄ (2.4000 g) showed that F₁ was mostly composed of some long-chain hydrocarbons and very minute quantities of some compounds within the aromatic region of the proton NMR. Fraction F₄ was a mixture of several sugar moieties. Fraction F₂ formed some insoluble solids at the bottom, which were filtered out. The filtrate of F₂ was rechromatographed with the same solvent system but at a 5% polarity increment, and sub-fractions were analysed on TLC and pooled together as F_{2.1}-F_{2.7}. Fraction F_{2.2} was subjected to Sephadex LH20 in chloroform: methanol (1:1) followed by preparative TLC on a coated glass plate in *n*-hexane: ethyl acetate (5.5:4.5) to afford 5.1 mg of compound (4). Sub-fractions F_{2.6.6}-F_{2.6.12} were subjected to preparative TLC on pre-coated glass plates of *n*-hexane: ethyl acetate (5.5:4.5) to afford 2.4 mg of compound (3). Some fractions within fraction F₃ precipitated upon exposure to open air in the fume hood and were filtered and washed off with appropriate solvents. Unfortunately, NMR analysis indicated artifacts in the solids. The filtrates were pooled together and chromatographed with the same solvent system at a 5% polarity increment. Fraction F_{3.14}-F_{3.20} was rechromatographed by isocratic elution with *n*-hexane: ethyl acetate:

methanol (55:45:4) and preparative TLC in *n*-hexane: ethyl acetate: methanol (55:45:4) afforded 2.3 mg of compound (2). Fractions F_{3.21} and F_{3.22} precipitated as white solids upon the addition of chloroform. They were carefully filtered and rinsed with solvent to afford 12 mg of compound (2). Fractions F_{3.24}-F_{3.31} were rechromatographed at a 2.5% polarity increment with *n*-hexane, ethyl acetate, and methanol. On analytical TLC with *n*-hexane: ethyl acetate (5.5:4.5), sub-fractions F_{(3.24 - F3.31) 4 - F_{(3.24 - F3.31) 11} appeared very close to the spotting zone while the other impurities moved up the plate. It was subsequently subjected to preparative TLC in the same solvent system to afford 4.4 mg of compound (1). Fraction F₃ produced at least six crystal shapes of different sugar (carbohydrate) moieties, with a very poor biological outcome for the present investigation. Fractions F₁-F₄ were subjected to an untargeted metabolomic investigation to identify other bioactive compounds distributed in minute amounts that were not isolated in this investigation.}

Spectroscopic data of 2a, 3β, 23-trihydroxy-17-norolean-12-ene, combrenorplatypta A (1)

Amorphous white solid (4.4 mg); *R*_f = 0.23 (*n*-hexane/ethyl acetate 2:8). [α]_D^{25.0} + 0.255° (*c* 0.1, MeOH); UV (MeOH) 210.35 nm, 1.981 Abs; FTIR: 3399, 2873, 2932, 1645.6 cm⁻¹; ¹H NMR (400 MHz, MeOD) δ 5.26 (1H, dd, ³*J*_{H,H} = 4.1 Hz, H-12), 3.71 (1H, td, ³*J*_{H,H} = 11.3, 5.0 Hz, H-2), 3.52 (1H, d, ²*J*_{a,b} = 11.1 Hz, H-23a), 3.37 (1H, d, ³*J*_{H,H} = 9.6 Hz, H-3), 3.29 (1H, d, ²*J*_{a,b} = 11.1 Hz, H-23b), 2.89 (1H, dd, ³*J*_{H,H} = 14.1, 4.6 Hz, H-18), 1.96 (1H, m, H-11a), 1.95 (2H, m, H-9, 1a), 1.84 (1H, m, H-15a), 1.71 (2H, m, H-19a, 17), 1.62 (2H, m, H-16), 1.55 (1H, m, H-21), 1.41 (1H, d, *J* = 2.5 Hz, H-22a), 1.31 (5H, m, H-5, 6, 7), 1.21 (1H, m, H-22b), 1.19 (3H, s, H-27), 1.14 (1H, m, H-19b), 1.07 (1H, m, H-15b), 1.05 (3H, s, H-25), 0.98 (1H, m, H-11b), 0.97 (3H, s, H-30), 0.92 (3H, s, H-29), 0.91 (1H, m, H-1b), 0.86 (3H, s, H-26), 0.72 (3H, s, H-24); ¹³C NMR (101 MHz, MeOD) δ 144.4 (C-13), 121.4 (C-12), 76.8 (C-3), 68.2 (C-2), 64.9 (C-23), 47.8 (C-17), 46.8 (C-5), 46.6 (C-9), 46.5 (C-1), 46.1 (C-19), 42.7 (C-4), 41.6 (C-18), 41.5 (C-14), 39.1 (C-8), 37.6 (C-10), 33.7 (C-22), 32.6 (C-21), 32.2 (C-29), 32.0 (C-7), 30.2 (C-20), 27.5 (C-15), 25.1 (C-27), 23.2 (C-11), 22.8 (C-16), 22.7 (C-30), 17.7 (C-6), 16.5 (C-26), 16.1 (C-25), 12.4 (C-24). ESIMS: *m/z* 444.3.

In vitro Antimicrobial Activity of Isolated Compounds

Fungi (*Cryptococcus neoformans* ATCC 208821, *Candida albicans* ATCC 10231, and *Candida glabrata* ATCC 2001) were obtained from the Department of Microbiology, University of Botswana. Each actively growing culture was standardised at 1.8 McFarland standards using a DensiCHEK (BioMerieux, Hazelwood, Missouri, USA). The MICs were determined according to the methods described by Hendiani and coworkers,¹² with some modifications as follows: different concentrations of the compounds were prepared by serial dilutions. The last two columns of sterile 96-well microplates were used as positive and negative controls. Sterile plates were used, and 125 μL of yeast extract peptone dextrose (YEPD) broth (Merck, Darmstadt, Germany) was introduced to each well under sterile conditions. The compounds (125 μL) were then introduced to each well and properly mixed with the YEPD broth using the multichannel micropipette. The positive, fluconazole (Merck), and negative controls were introduced to their respective wells, followed by 10 μL of the respective organisms in each well. All samples were incubated for 24 hours at 37 °C, after which the results were taken. The MICs were determined with the addition of 50 μL of 0.2 mg/mL 3-(4, 5-dimethylthiazol-2-yl)-2,5-diphenyltetrazolium bromide (MTT) to each well after incubation.

Density Functional Theory (DFT) and Time-Dependent Density Functional Theory (TD-DFT) calculations

The DFT and TD-DFT calculations were performed using the B3LYP¹³ hybrid functional together with Grimme's dispersion correction¹⁴ and 6-311++G** basis set.¹⁵ The integral equation formalism polarisable continuum model (IEFPCM) together with methanol was employed to mimic the experimental conditions. The optimised geometries were confirmed to be real minima on the potential energy surface with no imaginary frequencies. The electronic circular dichroism (ECD) spectra were calculated using TD-DFT by considering a total of 250 states. The

calculated ECD wavelengths were red-shifted by 30 nm for better comparison with the corresponding experimental spectra. All the calculations were performed using the Gaussian program package (version G16-A.03).¹⁶

Molecular Docking Studies

The molecular docking studies of the compounds and the positive control were performed using the AutoDock software¹⁷ against the active sites of the protein 14 α -demethylase of *Candida albicans* (PDB: 5TZ1). All the geometries of the ligand and its metal complexes used for the docking calculations were optimised using DFT calculations and converted to PDB files using the Gaussview software, whereas the PDB file for 14 α -demethylase of *Candida albicans* was downloaded from the Protein Data Bank (PDB: 5TZ1). The co-crystallised substrate and water molecules were removed from the receptor using the MGL 1.5.6 software. After cleaning the protein, only polar hydrogens were added, together with the Kollman charges. The grid box was constructed using 100, 100, and 100 pointing in the x, y, and z dimensions, respectively, with a grid point spacing of 0.375 Å. The center grid box was set¹⁸ at 62.594, 66.774, and 2.688 Å for the x, y, and z centers, respectively. The total number of genetic algorithms was set at 100, which generated one hundred different conformations for each of the molecules. No convergence problem was encountered during the calculations. The conformers with the lowest binding free energies were used for the visualisation of the interactions between the active amino acids and the molecule using the Discovery Studio software.

Results and Discussion

Following the traditional uses and metabolomic study,⁸ pre-isolation analysis of the extracts of *C. platypetalum* by bioactivity informed the present bioguided isolation of compounds. The methanol (MeOH) extract of the root displayed a MIC value of 0.0625 mg/mL against *Candida albicans* ATCC 10231 and *Candida glabrata* ATCC 2001, and a MIC value of 0.5 mg/mL against *Cryptococcus neoformans* ATCC 208821 at $P = 0.0002$. The extract was subsequently chromatographed repeatedly by silica gel column, Sephadex LH20, and preparative thin-layer chromatography. The fractions of the extract were simultaneously bio-investigated until the most potent fractions afforded combrenorplatypta A (1) and three other (Figure 1) active compounds (2-4).

Spectrometric and Spectroscopic Study of Isolated Compounds

Compound (1) chemical formula of C₂₉H₄₈O₃ was confirmed from its ESIMS spectrum, which showed an exact mass of m/z : 444.3, [M+1]⁺ 445.3. The degree of unsaturation of compound (1) was calculated from the deduced chemical formula and found to be six. FTIR peaks at 3399 (OH), 2932 (-CH₃ asym. str.), 2873 (-CH₃ sym. str.), and 1645 (C=C) cm⁻¹ were observed.

The proton NMR spectrum of (1) indicated the vicinal relationship of two oxymethine protons. One of the oxymethine protons resonated at

3.71 ppm (td, ³J_{H,H} = 11.3, 5.0 Hz, 1H) and showed coupling with protons at C-1 and C-3. The other oxymethine proton showed a peak at 3.37 ppm (d, ³J_{H,H} = 9.6 Hz) and was coupled with the oxymethine proton at C-2. The proton relationships described above were confirmed with the ¹H-¹H COSY cross-peaks displayed at the frequency F2 axis of one proton and the frequency F1 axis of its coupling proton. Both vicinal protons at 3.71 ppm (C2) and 3.37 ppm (C3) formed an AB part of an ABMX spin system. The chirality center at C4 downfield 42.7 ppm induced the diastereotopic protons (anisochronous, downfield 3.29 ppm and 3.52 ppm) at C-23 downfield 64.9 ppm on the carbon spectrum to split each other with a homonuclear germinal coupling to give an AB_q with a leaning or roofing effect, $\delta_a = 3.29$ ppm, $\delta_b = 3.52$ ppm (AB_q, 2H, ²J_{a,b} = 11.1 Hz) from experimental deductions. By calculations, $\delta_a = 3.28$ ppm, $\delta_b = 3.52$ ppm (AB_q, 2H, ²J_{a,b} = 11.2 Hz), $\Delta V_{ab} = 0.23$ ppm, and M = 3.40 ppm, peak intensity ratios of 1:1.27:1.27:1 reflecting the roofing effect confirm an AB_q. The above observations and the presence of a double doublet at 2.89 ppm (dd, ³J_{H,H} = 14.1, 4.6 Hz) coupling to protons at C-19 (downfield 41.6 ppm) account for the axial-axial and axial-equatorial (homonuclear) coupling interactions between the proton of C18 and the protons of C19 and confirm the norolean-12-ene structural backbone.

The carbon spectrum for compound 1 displayed twenty-nine (29) carbon peaks. Endocyclic olefinic methine carbon appeared downfield at 121.6 ppm (C12) and correlated with the diagnostic proton at 5.26 ppm. The assignment of methyl (six singlet protons) groups was based on HMBC correlations (Figure S1a, Figure S1b, and Table S1, respectively). The OH at C2 was deduced from the diaxial (H-2_{ax}/H-1_{ax}) coupling constant (³J_{H,H} = 11.3; 5.0 Hz, H-2) to be equatorial. The OH at C3 attached to the carbon resonating downfield at 76.8 ppm is axial (trans-related to the OH at C2). The C3 proton displayed HMBC (³J_{H,c}) correlations (Figure S1a-S1b) with C1, C23, and C24, which informed the substituent location and structural arrangements of ring A. The rings and carbon numbering are presented in Figure S1b. The equatorial location of the primary hydroxyl group at C23 was further supported by its 64.9 ppm downfield shift resonance.¹⁹ The presence of ten sp³ methylene carbons, six sp³ methyl groups, six sp³ methine, and one sp² methine carbon was confirmed (Figures S1a and S1b). The methyl and methine signals appeared positive, while the methylene signals appeared negative on DEPT 135. The methyl carbons were further confirmed by the DEPT 90 experiment. The proton and carbon spectra in combination confirmed the diagnostic peaks consistent with the norolean-12-ene pentacyclic triterpenoid backbone.

The relative stereochemistry of C2 and C3 was confirmed to be 2 α , and 3 β based on the analysis of the coupling constants.²⁰ This is consistent with the selected NOESY correlations between H2 and H24, H2, and H25, and H24 and H25, respectively (Figures S1a and S1b). The absolute configuration of compound (1) was determined to be 2R, 3R, 4R, 5R, 8R, 9R, 10R, 14S, 17S, and 18R (Figure S1b) by electronic circular dichroism (ECD) spectroscopy and time-dependent density functional theory (TD-DFT) calculations.

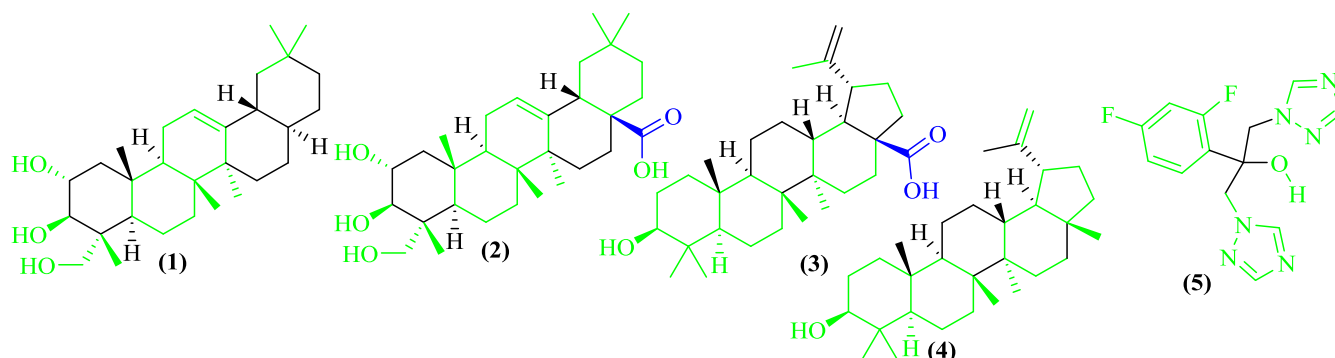


Figure 1: Structures of bioguided isolated compounds (1-4) from *Combretum platypetalum* and fluconazole (5). The pharmacophore is indicated by a green highlight. The blue highlight indicates a hydrophilic fragment that possibly deactivates sufficient binding to the target site and reduces the activity of the molecule against fungal pathogens

The ECD spectrum generated the curve with the observed positive and negative cotton effects (CE) for compound (1) and its stereoisomer in Figure 2. Other stereochemical comparisons for compound (1) have been presented in the supplementary section of Figure S1c.

In the computational study of compound 1, all experimental proton and carbon chemical shift assignments were computationally confirmed by TD-DFT calculations. A correlation between the assigned experimental and computational chemical shifts was observed, with an R^2 value of 0.8872 for compound 1 (Figure S1d). In comparison with literature reports, the carbon chemical shifts for (1) were in agreement with literature values for the closely related compounds,^{21, 22} of the olean-12-ene pentacyclic triterpenoids (Table S1). Compound (1) was thus concluded to be a 17-nor pentacyclic triterpenoid, trivially named combrenorplatypta A (2 α , 3 β , 23-trihydroxy-17-norolean-12-ene pentacyclic triterpenoid). Compound (1) was first patented in 2021.²³ This is its first spectroscopic description and its first occurrence in the genus. Except for the absence of a methyl group at C17, the ^1H and ^{13}C spectroscopic data are similar to those of other pentacyclic triterpenoids of the oleanane structural backbone.¹⁹ The loss of the methyl group is expected to have occurred through the biosynthetic action(s) of cytochrome P450 enzymes.²⁴ *Combretum quadrangulare* provided the first evidence of a nortriterpenoid for genus.^{25, 26} However, this is not the first report of the occurrence of nor-oleanane pentacyclic triterpenoids^{27, 28} in nature. Compounds (2),^{21, 22} (3),²⁹ and (4)^{30, 31} have been previously described (Figures S2 to S4). However, the ECD spectrum of compound (2) is presented for the first time, to the best of our knowledge. All compounds are identified with the species for the first time. Structures (2-4) were previously identified within the genus and family³²⁻³⁴ of the species.

In vitro and Computational Antifungal Activity Investigation of Isolated Compounds

The present investigation was focused on *C. albicans*, a yeast that poses more health challenges in terms of the number of new infections and co-infections in immunocompromised patients,^{35, 36} and deaths. The recent drug-resistant strains of *C. albicans*, particularly to fluconazole and other azole drugs, are worrisome and have been linked to the overexpression and mutation of the drug target, the ergosterol

biosynthesis gene *ERG11*.^{37, 38} The *ERG11* gene encodes lanosterol demethylase,³⁹ which upon mutation results in amino acid substitution³⁹ and, subsequently, the binding interaction between the drug and the target is disrupted, leading to the observed resistance. The current studies explored the biodiversity of nature and its traditional healing properties in search of new agents that could curb the growing concern about the resistance to available antifungal agents. The least active of the natural compounds in the present study displayed at least sixfold the activity of fluconazole against *C. albicans*, both in the *in vitro* investigation and the computational studies (Figure 3 and Table S2). The *in vitro* investigated compounds (1, 2, and 4) showed MIC values of 2.92 μM , 15.96 μM , and 2.30 μM , respectively, against *C. albicans*. This is in strong agreement with a previous report where a mixture of asiatic acid and arjunolic acid (2), isolated from *Combretum nelsonii*, produced a MIC value of 0.9 $\mu\text{g mL}^{-1}$,⁴⁰ comparable with the reported control, amphotericin B, against *C. albicans*. The reported MIC value for compound (2) in Figure 3 against *C. neoformans* also agrees with the reported literature-reported MIC value of 0.4 $\mu\text{g mL}^{-1}$.⁴⁰

The computational study against *C. albicans* (PDB: 5TZ1) indicates that compounds (1-4) need as low as -10.64, -9.96, -10.00, and -10.74 kcal/mol, respectively, for sufficient binding to the sterol 14 α -demethylase active sites to completely inhibit it from interactions with lanosterol and subsequently interrupt the biosynthesis pathway of ergosterol. The computed docking score inhibition constant (K_i) values were 15.93 nM, 49.86 nM, 47.02 nM, and 13.48 nM for compounds (1-4), respectively, where other experimental variation influences have been placed under control (Table S2). From the computational study, the most active compound is 4, followed by 1, 3, and 2. These are in strong agreement with the *in vitro*-investigated compounds (Figure 3). Comparatively, fluconazole required a higher binding energy of -6.79 kcal/mol to sufficiently interact with the sterol 14 α -demethylase active sites for inhibition of the biosynthesis of ergosterol, at a computed docking score of 10.57 μM inhibition constant (K_i), and *in vitro* MIC value of 102.19 μM . All *in vitro*-investigated natural compounds showed potency better than fluconazole against *C. albicans* and *C. neoformans*. Except for compound (1), compounds (2) and (4) elicited slightly better activity relative to fluconazole against *C. glabrata* (Figure 3).

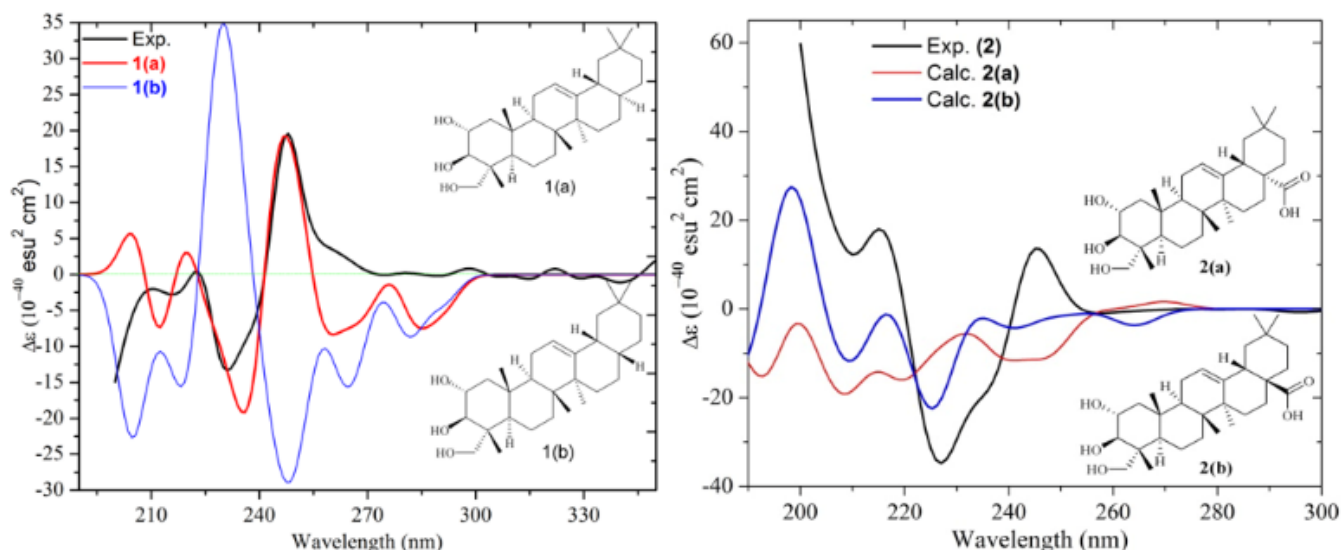


Figure 2: Experimental and TD-DFT calculated ECD spectra and 2D view of Compound 1 (a) rings D and E trans fused (b) rings D and E cis fused; Compound 2 (a) rings D and E trans fused (b) rings D and E cis fused; In the supplementary document, spectra of other stereochemical isomers for compound 1 have been presented

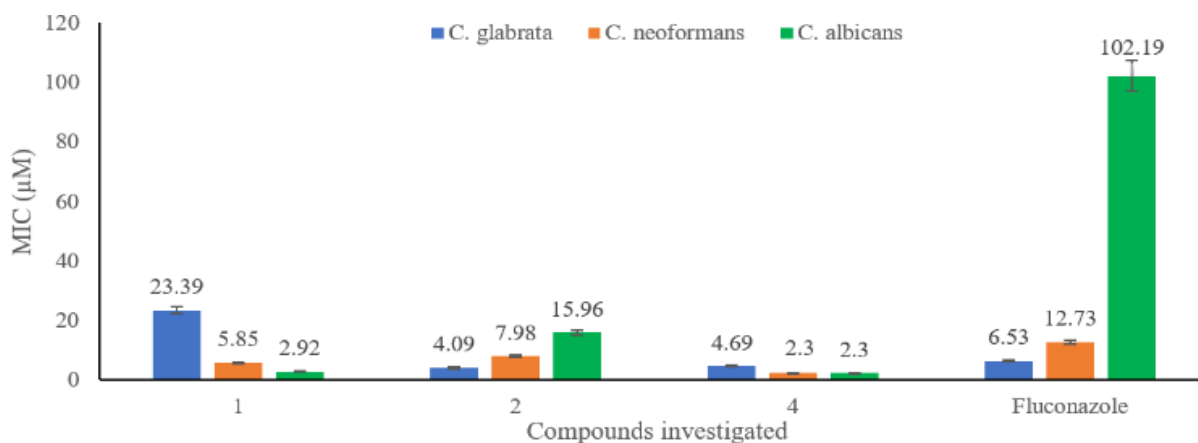


Figure 3: Comparison of the *in vitro* antifungal MICs ($P < 0.05$) of bioguided isolated compounds (1), (2), and (4) relative to a standard drug currently in use; Compounds (3) were in limited quantities and thus could not be captured in this presentation; Compound (2) performed best against *C. glabrata*, and compound (4) against *C. neoformans* and *C. albicans*.

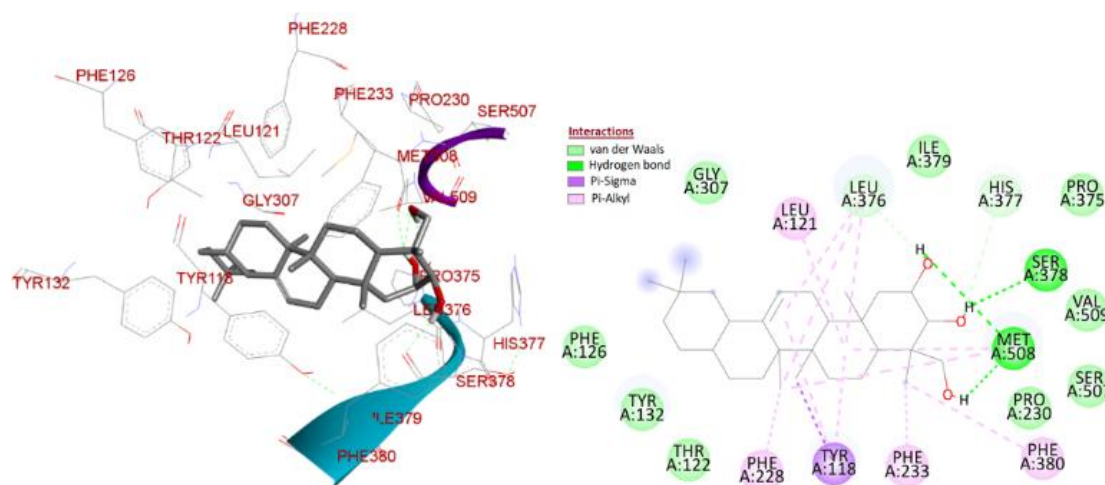


Figure 4a: The binding interactions of compound (1) against sterol 14 α -demethylase; binding energy of -10.64 kcal/mol and inhibition constant (K_i) of 15.93 nM.

Structure-Activity Relationship and Molecular Docking

All compounds have fewer than five hydrogen bond donors, less than ten hydrogen bond acceptors, and a molecular weight of less than 500 Da, which are the basic highlighted parameters for a drug-like candidate,⁴¹ provided other physicochemical parameters in a future study agree with the requirements. Rings B, C, and E of the oleanane-type pentacyclic triterpenoids appeared to bear the most active parts of the molecules against the sterol 14 α -demethylase. The same applies to rings A, B, D, and E of the lupine-type pentacyclic triterpenoid (Figures 1 and 4a-4b/ S5a- S5c).

The absence of the C17 carboxylic acid linkage in the pentacyclic triterpenoids led to a pronounced increase in observed biological activity, both in the *in vitro* and computational studies. This opens up a new area of research to investigate the influence of C17 substitution (and maybe other substitution patterns) of pentacyclic triterpenoids on the biological activity against fungal pathogens via the ergosterol biosynthetic pathway. Compounds (3) and (4) are more lipophilic compared to their other triterpenoid counterparts (1) and (2). Hence, they are expected to possess better binding affinities to the protein, be more bioavailable in the *in vivo* study, and also elicit more activity at therapeutic doses.

Except for compound (2), which had no π - σ / π - π interaction, all compounds exhibited H-bonding, pi sigma (π - σ / π - π), van der Waals, and pi alkyl (π -alkyl) interactions with the sterol 14 α -demethylase (Figures 4a-b, Figures S5a-c), and this is also summarised in Table S2. There is the possibility that the five-membered cyclic nature of ring E of the lupine-type pentacyclic triterpenoids influences the slightly

higher biological activity observed between (4 and 1) and between (3 and 2), respectively, in addition to the lipophilic nature of (3 and 4). The root mean square deviation (RMSD) of the ligands from their reference positions in the ligand-receptor complex after docking for compounds (1-4) was 0.26, 0.14, 0.51, and 0.17, respectively. The toxicity studies of the compounds at therapeutic doses should be investigated to confirm that they do not interfere with cholesterol biosynthesis and are not toxic to the human host cells. The best and safest route of administration should also be investigated in the animal pre-clinical study, even though some slight variations might exist in humans. It would, however, provide a guide for the subsequent clinical study when it sails through the preclinical filter.

Conclusion

Combretum platypetalum has produced potential antifungal lead compounds (1-4). All four compounds surpass fluconazole in binding affinity to the sterol 14 α -demethylase target, using *C. albicans* (PDB: 5TZ1) as a reference fungal pathogen. The MIC values ranged from 4 nM to 49.86 nM from molecular docking and 2.30 μ M to 15 μ M for *in vitro* bio-investigated isolated compounds. The isolated compounds may elicit antifungal activity by interrupting the ergosterol biosynthetic pathway from our molecular docking study, which subsequently leads to fungal cell death. Future pre-clinical investigations should involve *in vivo* assays, toxicity studies, *in-vivo-in vitro* correlation studies, animal pharmacokinetic profiling, and the bioavailability of compounds (1-4) against fungal pathogens.

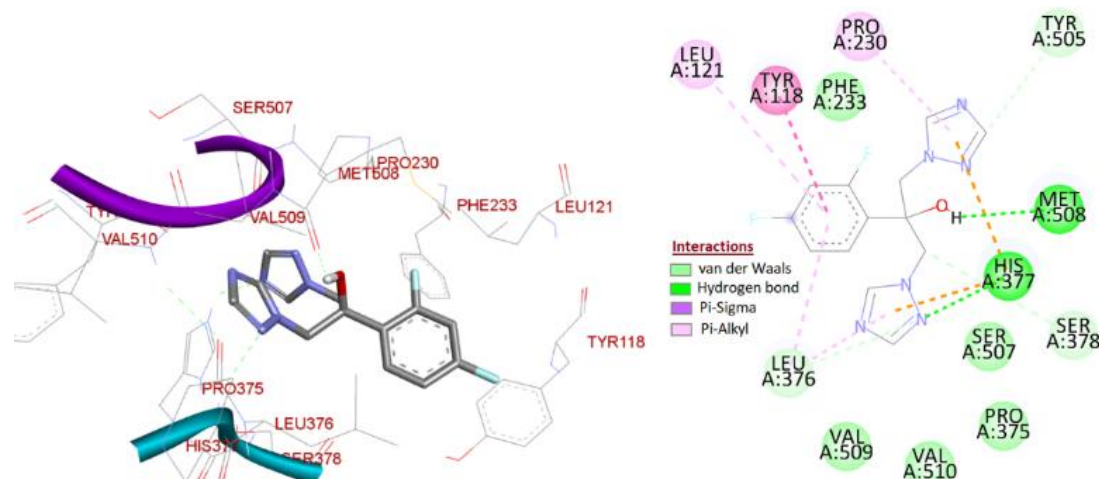


Figure 4b: The binding interactions of fluconazole against sterol 14 α -demethylase; binding energy of -6.79 kcal/mol and inhibition constant (K_i) of 10.57 μ M

Conflict of Interest

The authors declare no conflict of interest.

Authors' Declaration

The authors hereby declare that the work presented in this article is original and that any liability for claims relating to the content of this article will be borne by them.

Acknowledgments

The Office of Research and Development, University of Botswana, is acknowledged for providing funding support to DL. Joseph Sarwuan Tarka University, Makurdi, formerly known as the University of Agriculture, Makurdi, Nigeria, is acknowledged for its funding support for SDU.

References

- Dauda M, Musa A, Ilyas M, Abdullahi M, Haruna A. Antimicrobial potential of 2', 4'-dihydroxy-4-prenyloxychalcone combined with ciprofloxacin and fluconazole. *Trop. J. Nat. Prod. Res.* 2019;3(9):277-81.
- Hosseini-Moghaddam SM, Ouédraogo A, Naylor KL, Bota SE, Husain S, Nash DM, Paterson, J M. Incidence and outcomes of invasive fungal infection among solid organ transplant recipients: a population-based cohort study. *Transpl. Infect. Dis.* 2020;22(2):e13250.
- Gupta AK, Venkataraman M. Antifungal resistance in superficial mycoses. *J. Dermatol. Treat.* 2022;33(4):1888-95.
- Jordá T, Puig S. Regulation of ergosterol biosynthesis in *Saccharomyces cerevisiae*. *Genes*. 2020;11(7):795.
- Lindo L, Cardoza RE, Lorenzana A, Casquero PA, Gutiérrez S. Identification of plant genes putatively involved in the perception of fungal ergosterol-squalene. *J. Integr. Plant Biol.* 2020;62(7):927-47.
- Meshcheryakova OL, Shuvaeva GP, Sviridova TV, Tolkacheva AA, Korneeva OS. Study of the Effect of Squalene Epoxidase Activity on Squalene Biosynthesis by Yeast *Saccharomyces Cerevisiae* VGS α -2. *KnE Life Sci.* 2022:491–500-491–500.
- McCarty KD, Sullivan ME, Tateishi Y, Hargrove TY, Lepesheva GI, Guengerich FP. Processive kinetics in the three-step lanosterol 14 α -demethylation reaction catalyzed by human cytochrome P450 51A1. *J. Biol. Chem.* 2023;299(7).
- Umoh SD, Bojase G, Masesane IB, Majinda RT, Sichilongo KF. Untargeted GC-MS metabolomics to identify and classify bioactive compounds in *Combretum platypetalum* subsp. oatesii (Rolfe) Exell (*Combretaceae*). *Phytochem. Anal.* 2023;34(1):127-38.
- Wende M, Sithole S, Fru CG, Stevens MY, Mukanganyama S. The Effects of Combining Cancer Drugs with Compounds Isolated from *Combretum zeyheri* Sond. and *Combretum platypetalum* Welw. ex MA Lawson (*Combretaceae*) on the Viability of Jurkat T Cells and HL-60 Cells. *Biomed. Res. Int.* 2021;2021.
- Machingauta A, Stevens MY, Fru CG, Sithole S, Yeboah S, Mukanganyama S. Evaluation of the antiproliferative effect of β -sitosterol isolated from *Combretum platypetalum* Welw. ex MA Lawson (*Combretaceae*) on Jurkat-T cells and protection by glutathione. *Adv. trad. med.* 2022:1-9.
- Lima GRdM, de Sales IRP, Caldas Filho MRD, de Jesus NZT, Falcão HdS, Barbosa-Filho JM, Cabral AGS, Souto AL, Tavares JF, Batista LM. Bioactivities of the Genus *Combretum* (*Combretaceae*): A Review. *Molecules*. 2012;17(8).
- Hendiani I, Susanto A, Carolina DN, Ibrahim R, Balafif FF. Minimum inhibitory concentration (MIC) and minimum bactericidal concentration (MBC) of mangosteen (*Garcinia mangostana* Linn.) rind extract against *Aggregatibacter actinomycetemcomitans*. *Padjadjaran J. Dent.* 2020;32(2):131-5.
- Stephens PJ, Devlin FJ, Chabalowski CF, Frisch MJ. Ab initio calculation of vibrational absorption and circular dichroism spectra using density functional force fields. *J. Phys. Chem.* 1994;98(45):11623-7.
- Grimme S, Furche F, Ahlrichs R. An improved method for density functional calculations of the frequency-dependent optical rotation. *Chem. Phys. Lett.* 2002;361(3-4):321-8.
- Krishnan R, Binkley JS, Seeger R, Pople JA. Self-consistent molecular orbital methods. XX. A basis set for correlated wave functions. *J. Chem. Phys.* 1980;72(1):650-4.
- Frisch MJ, Trucks GW, Schlegel HB, Scuseria GE, Robb MA, Cheeseman JR, Montgomery Jr JA, Vreven T, Kudin KN, Burant JC, Millam JM, Lyengar SS, Tomasi J, Barone V, Mennucci B, Cossi M, Scalmani G, Rega N, Petersson GA, Nakatsuji H, Hada M, Ehara M, Toyota K, Fukuda R, Hasegawa J, Ishida M, Nakajima T, Honda Y, Kitao O, Nakai H, Klene M, Li X, Knox JE, Hratchian HP, Cross JB, Bakken V, Adamo C, Jaramillo J,

- Gomperts R, Stratmann RE, Yazyev O, Austin AJ, Cammi R, Pomelli C, Ochterski JW, Ayala PY, Morokuma K, Voth GA, Salvador P, Dannenberg JJ, Zakrzewski VG, Dapprich S, Daniels AD, Strain MC, Farkas O, Malick DK, Rabuck AD, Raghavachari K, Foresman JB, Ortiz JV, Cui Q, Baboul AG, Clifford S, Cioslowski J, Stefanov BB, Liu G, Liashenko A, Piskorz P, Komaromi I, Martin RL, Fox DJ, Keith T, Al-Laham MA, Peng CY, Nanayakkara A, Challacombe M, Gill PMW, Johnson B, Chen W, Wong MW, Gonzalez C, Pople JA. Gaussian 16. Revision 01 ed. Wallingford CT: Gaussian, Inc.; 2016.
17. Bitew M, Desalegn T, Demissie TB, Belayneh A, Endale M, Eswaramoorthy R. Pharmacokinetics and drug-likeness of antidiabetic flavonoids: Molecular docking and DFT study. *Plos one*. 2021;16(12):e0260853.
 18. Hargrove TY, Friggeri L, Wawrzak Z, Qi A, Hoekstra WJ, Schotzinger RJ, York JD, Guengerich FP, Lepesheva GI. Structural analyses of *Candida albicans* sterol 14 α -demethylase complexed with azole drugs address the molecular basis of azole-mediated inhibition of fungal sterol biosynthesis. *J. Biol. Chem.* 2017;292(16):6728-43.
 19. Mahato SB, Kundu AP. ¹³C NMR spectra of pentacyclic triterpenoids—a compilation and some salient features. *Phytochemistry*. 1994;37(6):1517-75.
 20. Ketut Adnyana, Yasuhiro Tezuka, Arjun H. Banskota, Quanbo Xiong, Kim Qui Tran, Shigetoshi Kadota. Quadranosides I-V, New Triterpene Glucosides from the Seeds of *Combretum quadrangulare*. *J. Nat. Prod.* 2000;63:496-500.
 21. Kundu AP, Mahato SB. Triterpenoids and their glycosides from *Terminalia chebula*. *Phytochemistry*. 1993;32(4):999-1002.
 22. Ichōron N, Tor-Anyiin TA, Igoli JO. Arjunolic Acid from the Root Bark of *Terminalia catappa* Linn: doi.org/10.26538/tjnpr/v2i11. 6. *Trop. J. Nat. Prod. Res.* 2018;2(11):494-7.
 23. Information NCFB. PubChem Compound Summary for CID 155081824. Retrieved March 17, 2023 from <https://pubchem.ncbi.nlm.nih.gov/compound/1550818242023>.
 24. Lee CF, Chen LX, Chiang CY, Lai CY, Lin HC. The biosynthesis of norsesquiterpene aculenes requires three cytochrome P450 enzymes to catalyze a stepwise demethylation process. *Angew. Chem., Int. Ed. Engl.* 2019;58(51):18414-8.
 25. Banskota AH, Tezuka Y, Tran KQ, Tanaka K, Saiki I, Kadota S. Thirteen novel cycloartane-type triterpenes from *Combretum quadrangulare*. *J. Nat. Prod.* 2000;63(1):57-64.
 26. Banskota AH, Tezuka Y, Tran KQ, Tanaka K, Saiki I, Kadota S. Methyl quadrangularates AD and related triterpenes from *Combretum quadrangulare*. *Chem. Pharm. Bull.* 2000;48(4):496-504.
 27. Jian-Feng Xu, Hui-Bin Wu, Ding-Cai Liu, Long Sha, Wen-Hui Wu, Hua Fan, Yi-Shan Song, Zhu HG. Three New 29 Carbon Skeletons Pentacyclic Triterpenoids and S-equal from Biogas Slurry. *Bull. Korean Chem. Soc.* 2015;36:2862–8.
 28. Higuchi R, Kawasaki T. Pericarp saponins of *Akebia quinata* Decne. II. Arjunolic and norarjunolic acids, and their glycosides. *Chem. Pharm. Bull.* 1976;24(6):1314-23.
 29. Egbubine CO, Adeyemi MM, Habila JD. Isolation and characterization of betulinic acid from the stem bark of *Feretia canthioides* Hiern and its antimalarial potential. *Bull. Natl. Res. Cent.* 2020;44(1):1-7.
 30. Sánchez-Burgos J, Ramírez-Mares M, Gallegos-Infante J, González-Laredo R, Moreno-Jiménez M, Cháirez-Ramírez M, Medina-Torres L, Rocha-Guzmán N. Isolation of lupeol from white oak leaves and its anti-inflammatory activity. *Ind. Crops Prod.* 2015;77:827-32.
 31. Hassan G, Zahra Q, Ali I, Engel N, Ali K, Bahreen G, Ahmad VU, Aziz S, Wang D. Anticancer Activity of Hispidulin from *Saussurea simpsoniana* and Lupeol from *Vincetoxicum arnottianum*: doi.org/10.26538/tjnpr/v4i2. 2. *Trop. J. Nat. Prod. Res.* 2020;4(2):31-5.
 32. Bisoli E, Garcez WS, Hamerski L, Tieppo C, Garcez FR. Bioactive pentacyclic triterpenes from the stems of *Combretum laxum*. *Molecules*. 2008;13(11):2717-28.
 33. Muhammad A, Hassan H, Sani Y, Jimoh A, Bakare L, Sadam A. Isolation and characterization of lupeol and stigmaterol from methanol root extract of *Combretum hypopolinum* (diels.) Okafor (*Combretaceae*). *J. Med. Pharm. Allied Sci.* 2021;18(4):3547-53.
 34. Facundo VA, Rios KA, Medeiros CM, Militão JS, Miranda ALP, Epifanio RdA, Carvalho MP, Andrade AT, Pinto AC, Rezende CM. Arjunolic acid in the ethanolic extract of *Combretum leprosum* root and its use as a potential multi-functional phytomedicine and drug for neurodegenerative disorders: anti-inflammatory and anticholinesterasic activities. *J. Braz. Chem. Soc.* 2005;16:1309-12.
 35. Ezeokoli OT, Gcilitshana O, Pohl CH. Risk factors for fungal co-infections in critically ill COVID-19 patients, with a focus on immunosuppressants. *J. Fungus*. 2021;7(7):545.
 36. Ndukwu C, Mbakwem-Aniebo C, Frank-Peterside N. Prevalence of *Candida* Co-Infections among Patients with Pulmonary Tuberculosis in Emuoha, Rivers State, Nigeria. *IOSR J. Pharm. Biol. Sci.* 2016;11(5):60-3.
 37. Jin L, Cao Z, Wang Q, Wang Y, Wang X, Chen H, Wang H. MDR1 overexpression combined with ERG11 mutations induce high-level fluconazole resistance in *Candida tropicalis* clinical isolates. *BMC Infect. Dis.* 2018;18:1-6.
 38. Dhasarathan P, AlSalhi MS, Devanesan S, Subbiah J, Ranjitsingh A, Binsalah M, Alfuraydi AA. Drug resistance in *Candida albicans* isolates and related changes in the structural domain of Mdr1 protein. *J. Infect. Public Health.* 2021;14(12):1848-53.
 39. Flowers SA, Colón B, Whaley SG, Schuler MA, Rogers PD. Contribution of clinically derived mutations in ERG11 to azole resistance in *Candida albicans*. *Antimicrob. Agents Chemother.* 2015;59(1):450-60.
 40. Masoko P, Mdee L, Mampuru L, Eloff J. Biological activity of two related triterpenes isolated from *Combretum nelsonii* (*Combretaceae*) leaves. *Nat. Prod. Res.*, 2008;22(12):1074-84.
 41. Protti ÍF, Rodrigues DR, Fonseca SK, Alves RJ, de Oliveira RB, Maltarollo VG. Do Drug-likeness Rules Apply to Oral Prodrugs? *ChemMedChem*. 2021;16(9):1446-56.